ACS APPLIED NANO MATERIALS

www.acsanm.org Article

E-Selectin Targeted Gold Nanoshells to Inhibit Breast Cancer Cell Binding to Lung Endothelial Cells

Z. Fereshteh, M.N. Dang, C. Wenck, E.S. Day, and J.H. Slater*

Cite This: https://doi.org/10.1021/acsanm.2c04967 Read Online

ACCESS | Metrics & More | Article Recommendations | Supporting Information

ABSTRACT: Extravasation of circulating tumor cells (CTCs) from the vasculature is a key step in cancer metastasis. CTCs bind to cell adhesion molecules (CAMs) expressed by endothelial cells (ECs) for flow arrest prior to extravasation. While a number of EC-expressed CAMs have been implicated in facilitating CTC binding, this work investigated the efficacy of inhibiting cancer cell binding to human lung microvascular ECs via antibody blocking of E-selectin using antibody-functionalized gold nanoshells (NS). The antibody-functionalized gold NS were synthesized using both directional and non-directional antibody conjugation techniques with variations in synthesis parameters (linker length, amount of passivating agents, and ratio of antibodies to NS) to gain a better understanding of these properties on the resultant hydrodynamic diameter, zeta potential, and antibody loading density. We quantified the ability of E-selectin antibody-functionalized NS to bind human lung microvascular endothelial cells (HMVEC-Ls) under non-inflamed and inflamed (TNF-α) conditions to inhibit binding of triple-negative MDA-MB-231s. E-selectin-targeted NS prepared using non-directional conjugation had higher antibody loading than those prepared via directional conjugation, resulting in the conjugates having similar overall binding to HMVEC-Ls at a given antibody concentration. E-selectin-targeted NS reduced MDA-MB-231 binding to HMVEC-Ls by up to 41% as determined using an *in vitro* binding assay. These results provide useful insights into the characteristics of antibody-functionalized NS prepared under different conditions while also demonstrating proof of concept that these conjugates hold potential to inhibit CTC binding to ECs, a critical step in extravasation during metastasis.

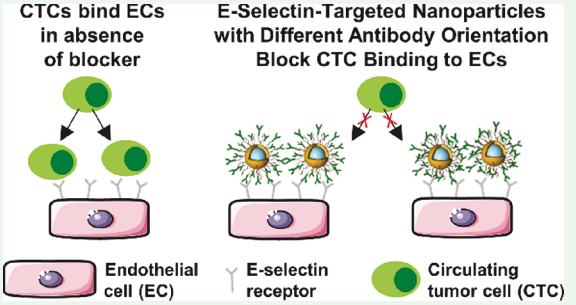

KEYWORDS: *circulating tumor cells, metastasis, nanomedicine, extravasation, nanoparticles, targeted therapy*

INTRODUCTION

Metastatic cancer is responsible for a vast majority of cancer-related deaths. This occurs when primary tumor cells disseminate into the vascular or lymphatic system to become circulating tumor cells (CTCs) that subsequently extravasate into other organs to form distant metastasis. While the mechanisms used during CTC extravasation are not fully understood, it is acknowledged that CTCs first adhere to blood vessel endothelial cells (ECs) through ligand−receptor interactions and then cross the vessel wall through transcellular or paracellular transport.[1−4] Several cell adhesion molecules (CAMs) expressed by ECs have been implicated in CTC binding, including endothelial leukocyte adhesion molecule-1 (E-selectin), vascular cell adhesion molecule-1 (VCAM1), and intercellular cell adhesion molecule-1 (ICAM1), all of which are upregulated by inflammatory cytokines.[5−7] Thus, inflammation plays a major role in enabling CTCs to bind ECs and extravasate into distant organs. This suggests that targeting CAMs that are upregulated by inflamed ECs could be a promising strategy to inhibit CTC binding and extravasation, either by enabling selective drug delivery to these sites or by blocking CTC/EC interactions. Here, we investigate the latter strategy using a nanomedicine-based approach to inhibit breast cancer cell binding to inflamed lung ECs *in vitro*.

Among the various types of cancers, breast cancer is among the most invasive.[8] One particularly aggressive subtype, triple-negative breast cancer (TNBC), exhibits earlier relapse and higher rates of metastasis than other subtypes, stemming from the fact that it is unsusceptible to currently available hormonal or targeted therapies.[9−12] Additionally, TNBC is unique in that, unlike other breast cancers that primarily spread to bone, it has a propensity to also metastasize to the lungs.[13] Therefore, we investigated the ability to inhibit TNBC cell binding to lung ECs using antibody-functionalized nanoparticles (NPs) targeting E-selectin. As noted above, E-selectin expression is upregulated by inflamed ECs and is engaged by CTCs to facilitate flow arrest and extravasation. Additionally, microvascular ECs in the bronchial mucosa constitutively

Received: November 15, 2022
Accepted: December 23, 2022

https://doi.org/10.1021/acsanm.2c04967
ACS Appl. Nano Mater. XXXX, XXX, XXX−XXX

Scheme 1. Directional and Non-Directional Conjugation of Antibodies to Nanoshells[a]

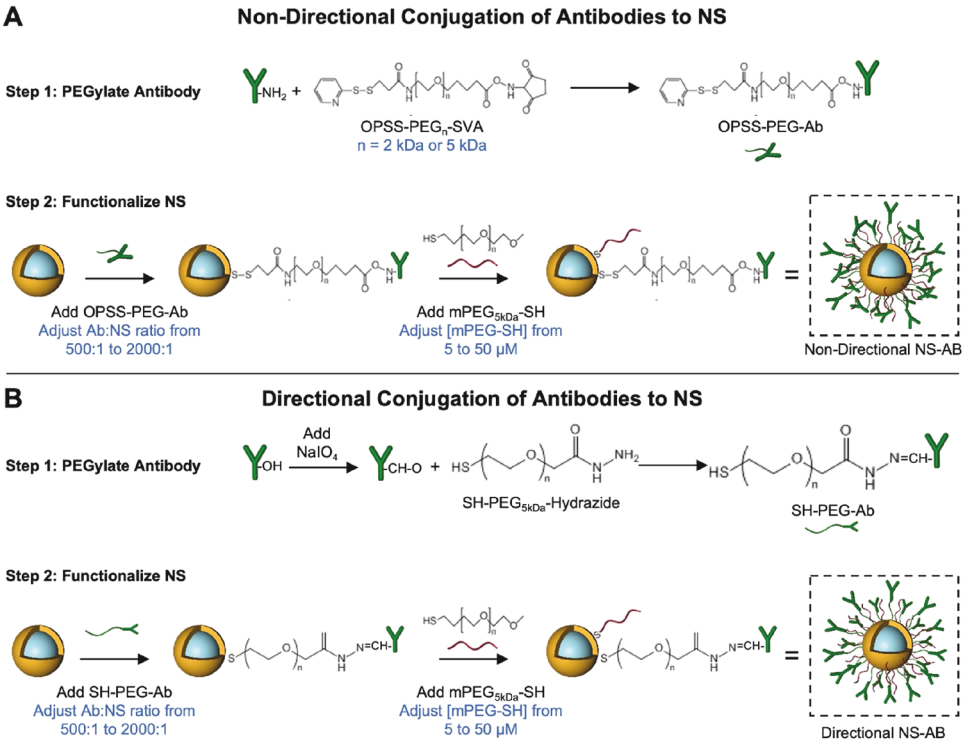

[a](A) Depiction of non-directional antibody attachment to NS using OPSS-PEG-SVA linkers. (B) Depiction of directional antibody attachment to NS using SH-PEG-hydrazide linkers. In both methods, NS were passivated with mPEG-SH after antibody conjugation. The blue font in (A) and (B) indicates the parameters that were varied to determine their influence on antibody loading density.

express E-selectin, which may contribute to the lung being a common site of metastasis.[3,14,15] Hence, we hypothesized that NPs designed to bind E-selectin on ECs could inhibit CTC binding to ECs through physical blockade of the receptors.

To investigate whether E-selectin-targeted NPs could inhibit TNBC interactions with lung ECs, we fabricated and characterized nanoshells (NS) functionalized with E-selectin antibodies. The NS are composed of a 120 nm diameter silica core surrounded by a ∼15 nm thick gold shell (total diameter ∼150 nm) and are well suited as a carrier platform for multiple reasons. First, and perhaps most importantly, their safety for human use has already been validated in clinical trials.[16−18] Second, the methods to attach antibodies to NS (and other gold-based NPs) are well established, supporting ease of bioconjugation. Third, NS have unique optical properties that enable them to be visualized with various imaging techniques.[19−21] Here, we exploit the ability of NS to emit two-photon-induced photoluminescence upon excitation with femtosecond pulsed 800 nm light to evaluate their binding to lung ECs using multiphoton microscopy.[19,22,23]

Several factors may impact the ability of antibody-functionalized NPs to bind target receptors on ECs to inhibit CTC binding. This includes the length of the linker used to attach the antibodies (which influences antibody accessibility and flexibility) as well as the density and directionality of the antibodies on the NP surface. Antibodies are typically conjugated to the surface of gold NPs using heterobifunctional poly(ethylene glycol) (PEG) linkers that contain a thiol or disulfide group at one end (to facilitate attachment to gold) and an *N*-hydroxysuccinimide (NHS), succinimidyl valerate (SVA), or a similar group at the other end (to facilitate binding to free amines present on antibodies).[24] While effective, this method results in non-directional antibody orientation, meaning that the antigen-binding region (Fab) of the antibody may face outward from the NP as desired, or it may face inward, rendering it less effective. An alternative approach is to functionalize NPs with antibodies using directional conjugation methods, such as a heterofunctional linker to bind the Fc region of a glycosylated antibody, allowing the Fab region to orient outward from the NP so that it is readily available to bind the target receptor.[25] Since the attachment chemistry and subsequent antibody orientation may affect the ability of antibody−NP conjugates to engage their target receptor, we directly compared a directional versus a non-directional conjugation method. We characterized antibody−NS conjugates prepared by each technique to gain a better understanding of the influence of various synthesis parameters (e.g., linker length, amount of passivating agents added, and ratio of antibodies/NS added) on the resultant NP hydrodynamic diameter, zeta potential, and antibody loading density (Scheme 1).

We also evaluated the ability of E-selectin antibody-functionalized NS to bind human lung microvascular endothelial cells (HMVEC-Ls) under both basal (non-inflamed) and inflamed (exposure to TNF-α) culture conditions. We found that E-selectin-targeted NS prepared using non-directional conjugation had higher antibody loading than those prepared via directional conjugation, resulting in the conjugates having similar overall binding to HMVEC-Ls at a given antibody concentration. Given that non-directional conjugation is simpler to perform, we evaluated the ability of non-directionally functionalized E-selectin-targeted NS to inhibit MDA-MB-231 cell binding to HMVEC-Ls and found that this approach was successful in both basal and inflamed

https://doi.org/10.1021/acsanm.2c04967
ACS Appl. Nano Mater. XXXX, XXX, XXX−XXX

conditions with up to 41% inhibition of 231 binding to lung ECs. These results provide useful insight into the characteristics of antibody−NP conjugates prepared under different synthesis conditions while also demonstrating *in vitro* proof of concept that antibody−NP conjugates hold potential as tools to inhibit CTC binding to lung microvascular ECs, a critical step in extravasation during the metastatic cascade.

EXPERIMENTAL SECTION

Synthesis of Gold NS. NS were synthesized as previously described by Oldenburg *et al.*[26] Briefly, 85 mM tetrakis-(hydroxymethyl)phosphonium chloride (THPC; Sigma-Aldrich, MO, USA), 29.7 mM chloroauric acid ($HAuCl_4$; Sigma-Aldrich, MO, USA), and 1 M sodium hydroxide (NaOH) prepared in Milli-Q water were combined and left to age at room temperature (RT) for ∼1−2 days to produce colloidal gold with a 2−3 nm diameter. The aging process was monitored using UV−visible spectrophotometry (Cary 60, Agilent Technologies, Santa Clara, CA, USA) to monitor the presence of a characteristic "bump" in the extinction spectra near 520 nm. The aged gold colloid and 1 M NaCl were added to 4% 3-aminopropyltriethoxysilane (3-APTES)-functionalized 120 nm diameter silica spheres (NanoComposix Co., San Diego, CA, USA) and the solution rocked for several days at RT to create "seed" consisting of silica cores coated with a low density of colloidal gold. The seed was purified by centrifugal filtration and resuspended in Milli-Q water to an absorbance of 1 at 530 nm (abs^{530nm} = 1; measured with the Cary 60 UV−visible spectrophotometer). The seed was mixed with formaldehyde and an aged solution of "Kcarb-gold", prepared by adding 12 mL of 29 mM $HAuCl_4$ and 200 mg of potassium carbonate to 800 mL of Milli-Q water, and leaving the solution in the dark for at least 8 h to reduce additional gold on the "seed" to form a complete gold shell. For each batch of NS, the ratio of seed, Kcarb-gold, and formaldehyde was adjusted to produce NS with a peak extinction near 800 nm and a dipole peak ($OD^{\sim 800nm}$) to trough ($OD^{\sim 530nm}$) ratio of greater than 3 (where OD = optical density). Following synthesis, NS were purified by centrifugation and diluted in Milli-Q water to the desired OD^{800nm} until use. NS were also visualized by transmission electron microscopy using a Zeiss Libra 120 transmission electron microscope (Figure S1).

PEGylation of E-Selectin or IgG Antibodies for Non-Directional Conjugation to NS. To non-directionally conjugate antibodies to NS, mouse anti-human E-selectin antibodies (CD62E, BBA16, R&D Systems, MN, USA) or goat anti-mouse IgG antibodies (AF007, R&D Systems, MN, USA) were incubated with 2 or 5 kDa orthopyridyl disulfide-PEG-succinimidyl valerate (OPSS-PEG_{2000}-SVA or OPSS-PEG_{5000}-SVA, Laysan Bio, Arab, AL, USA) in 100 mM sodium bicarbonate. Volumetrically, nine-parts OPSS-PEG-SVA in sodium bicarbonate was reacted with one-part antibody at a 2:1 (PEG/antibody) molar ratio, followed by rocking overnight at 4 °C. The volume was filtered through a 10 kDa molecular weight cutoff (MWCO) centrifuge filter (UFC801024, Sigma-Aldrich, MO, USA) at 2000*g* at 4 °C. After an additional HEPES wash, the solution was resuspended in HEPES and the protein concentration measured by reading the absorbance at 280 nm with a SYNERGY H1 microplate reader using a Take3 plate. The PEGylated antibodies were aliquoted and stored at −20 °C.

PEGylation of E-Selectin or IgG Antibodies for Directional Conjugation to NS. The protocol of Kumar *et al.* was utilized to prepare PEGylated antibodies for directional attachment to NS.[25] Specifically, 100 μL of 1 mg/mL mouse anti-human E-selectin antibodies (CD62E, BBA16, R&D Systems, MN, USA) or goat anti-mouse IgG antibodies (AF007, R&D Systems, MN, USA) diluted in Milli-Q water were incubated with 10 μL of 100 mM freshly made $NaIO_4$ (311448, Sigma-Aldrich, MO, USA) in the dark for 30−45 min at RT. To verify carbohydrate oxidation, 5 μL of the antibody solution was added to 15 μL of freshly prepared 10 mg/mL Purpald (162892, Sigma-Aldrich, MO, USA) solution. The color change to purple indicated the presence of aldehydes validating carbohydrate oxidation. The antibody solution was quenched with 5× volume of 1× PBS. Two microliters of 46.5 mM thiol-PEG_{5000}-hydrazide (HE003019-5K, Biochempeg Scientific Inc., MA, USA) was added to the solution and incubated for 1 h at RT. One milliliter of 40 mM 4-(2-hydroxyethyl)-1-piperazineethanesulfonic acid (HEPES) was added and the entire volume was filtered through a 10 kDa MWCO centrifuge filter (UFC801024, Sigma-Aldrich, MO, USA) at 2000*g* at 4 °C. After an additional HEPES wash, the solution was resuspended in HEPES and the protein concentration measured by reading the absorbance at 280 nm with a SYNERGY H1 microplate reader using a Take3 plate. PEGylated antibodies were aliquoted and stored at −20 °C until use.

Functionalization of NS with PEGylated Antibodies and mPEG-SH. PEGylated antibodies prepared using directional or non-directional conjugation were added to NS at ratios ranging from 500 to 2000 antibodies per NS and incubated at 4 °C for 4 h. The conjugates were vortexed and sonicated every hour during the 4 h incubation to prevent aggregation. To passivate the antibody−NS conjugates, 5 kDa methoxy-PEG-thiol (mPEG-SH, JenKem, Plano, TX, USA) was added to the samples, followed by rocking overnight at 4 °C. To determine the influence of mPEG-SH concentration on the resultant zeta potential and antibody loading density of the NS, mPEG-SH was added at concentrations ranging from 0 to 100 μM. NS functionalized with only mPEG-SH (NS-PEG) were prepared as a control. After overnight incubation with mPEG-SH, the conjugated NS were purified twice by centrifugation (1500*g* for 5 min) to pellet the NPs and remove excess unbound molecules with the supernatant, followed by resuspension in molecular biology grade water and storage at 4 °C.

Characterization of NS Properties. Bare NS, NS-AB (antibody-functionalized NS), and NS-PEG were characterized by UV−vis spectrophotometry (Cary 60, Agilent), dynamic light scattering (DLS), and zeta potential measurements (Litesizer 500, Anton Paar) to quantify their optical properties, hydrodynamic diameter, and surface charge. To acquire UV−vis spectra, a baseline was established by scanning water in a disposable cuvette with a wavelength range of 1000−400 nm at a scan speed of 2400 nm/min. NS were analyzed on the spectrophotometer to determine the extinction profile and the NS concentration was calculated from the peak extinction of each sample (OD^{800nm}) using Beer's law and the theoretical extinction coefficient of NS with 120 nm diameter silica cores and 15 nm thick gold shells. If necessary, stock solutions of NS were diluted in water to the desired working concentration. For DLS and zeta potential measurements, 500 μL of NS diluted in water to OD^{800nm} = 1 (2.8×10^9 NS/mL) was placed into Litesizer cuvettes or Omega cuvettes, respectively, and the samples were measured using a Litesizer 500. DLS measurements included 60 replicates, while zeta potential measurements included 1000 replicates.

Quantification of Antibody Loading on NS. The mean number of E-selectin antibodies loaded per NS was quantified using an on-particle enzyme-linked immunosorbent assay (ELISA).[27,28] The 2.8×10^9 NS-AB/mL (OD^{800nm} = 1) were incubated with 100 μg/mL horseradish peroxidase-labeled (HRP) goat anti-mouse IgG (HAF007, R&D Systems, MN, USA) secondary antibodies in 3% PBSA (3% bovine serum albumin in phosphate-buffered saline) for 1 h at RT in the dark. The samples were purified three times via centrifugation with 3% PBSA to remove excess secondary HRP antibodies, and the supernatant was collected to subtract background signal. The samples were incubated with 3,3′,5,5′-tetramethylbenzidine solution (TMB Core, BUF056A, Bio-Rad Laboratories, CA, USA) at RT and the reaction stopped with 2 M sulfuric acid after 10 min. The absorbance at 450 nm was measured using a SYNERGY H1 microplate reader, compared to a standard curve with known HRP secondary antibody concentrations, and the average number of antibodies per NS calculated by dividing the measured number of antibodies in the sample by the known number of NS in the sample.

Evaluating E-Selectin Antibody-Targeted NS Binding to Basal or Inflamed Lung Microvascular Endothelial Cells. Non-pooled human lung microvascular endothelial cells (HMVEC-Ls) (CC-2527, Group Ltd., Basel, Switzerland) were cultured in tissue-culture flasks in EGM-2MV BulletKit medium (CC-3156 and CC-

https://doi.org/10.1021/acsanm.2c04967
ACS Appl. Nano Mater. XXXX, XXX, XXX−XXX

4147, Group Ltd., Basel, Switzerland) at 37 °C and 5% CO_2. Cells were passaged between flasks or into sample plates when they reached 90% confluence by adding 3.0 mL of 0.25% trypsin at 37 °C for 3 min. The detached cells were collected, centrifuged to remove excess trypsin, suspended in EGM-2MV (Lonza, CAT # CC-3202), and seeded in 4-well chamber slides at a density of ~25,000 cells/cm^2. After reaching 90% confluency, HMVEC-Ls were labeled with 15 μM CellTracker Red (Thermo Fisher, CAT # C34552) for 30 min at 37 °C and 5% CO_2, followed by washing 3× with pre-warmed 1× PBS. All flasks and chamber slides were coated with 10 μg/mL fibronectin from human plasma (FN, F2006, St. Louis, MO, USA) prior to cell seeding.

To induce inflammation, HMVEC-Ls were activated with 500 μL of tumor necrosis factor alpha (10 ng/mL TNF-α, 10602-HNAE, Sino Biological Inc., PA, USA) for 6 h at 37 °C (referred to as inflamed samples) and washed 3× with pre-warmed 1× PBS (Scheme 2A). Inflammation was confirmed by measuring E-selectin expression

Scheme 2. Experimental Overview[a]

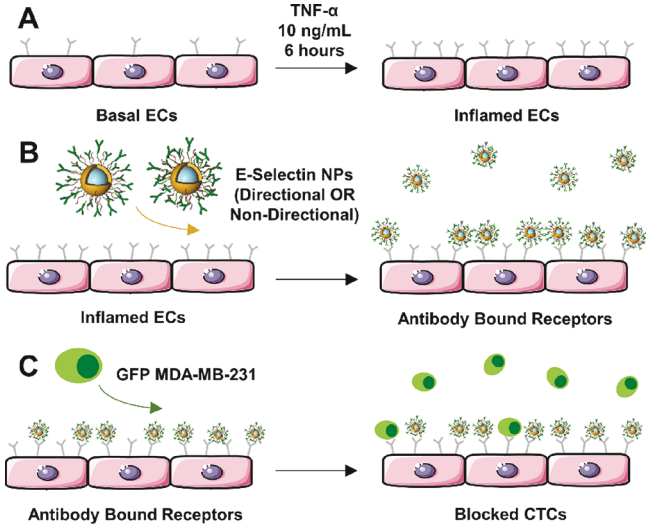

[a](A) Basal (non-inflamed) human lung microvascular endothelial cells (ECs) were incubated with TNF-α at 10 ng/mL for 6 h to induce inflammation and increase expression of E-selectin (depicted in gray). (B) Basal and inflamed ECs were treated with either directionally or non-directionally conjugated E-selectin NS to compare binding efficiencies between the two types of conjugation methods. For simplicity, only inflamed ECs are depicted, and the directional and non-directional NPs are shown together (in experiments, cells received one NP type at a time). (C) Following treatment with non-directional NS, basal and inflamed ECs were exposed to GFP-expressing MDA-MB-231s (231s) to quantify the ability of E-selectin-functionalized NS to inhibit the 231s from binding to ECs. For simplicity, only inflamed ECs are depicted.

using immunofluorescence labeling and imaging as described in the Supporting Information (Figure S4). Basal or inflamed ECs were incubated with 500 μL of one of the following solutions (three replicates per condition): (i) non- or directionally conjugated anti-E-selectin-functionalized NS prepared at AB/NS ratios ranging from 500 to 2000, (ii) non- or directionally conjugated anti-IgG-functionalized NS, or (iii) NS-PEG, with all NS types suspended in EGM-2MV media at a concentration of ~1.4 × 10^{10} NS/mL (OD^{800nm} = 5) (Scheme 2B). Cells were incubated in these solutions for 1 h at 37 °C and 5% CO2, washed 3× with pre-warmed 1× PBS to remove any unbound NS, fixed with 4% formaldehyde, and rinsed 3× with 1× PBS. After fixation, the chamber walls were removed and the cells counterstained with DAPI in Prolong Gold and stored at 4 °C. The slides were imaged using a Zeiss LSM 880 multiphoton microscope equipped with a Chameleon Vision II Ti:S pulsed laser (Coherent) operating at 80 MHz with a 140 fs pulse width. NS were imaged with the laser tuned to the NS peak resonance wavelength (~800 nm) at an average power of 1 mW using a 20× objective in combination with a long-pass dichroic mirror to collect photoluminescence from the NS (spanning a range from ~450 to 650 nm). Each condition was replicated three times, with each sample imaged in at least three locations. Cells were imaged in each corresponding region of interest with excitation/emission of 405/453 nm to visualize DAPI/nuclei and of 577/602 nm to visualize CytoTracker Red. The integrated intensity of each image was measured using ImageJ software and normalized to the number of cells and the intensity of the IgG-treated samples.

Inhibiting MDA-MB-231 Docking to HMVEC-L Using E-Selectin-Targeted NS. The ability to inhibit MDA-MB-231 binding to HMVEC-Ls using E-selectin-targeted NS was evaluated (Scheme 2C). Green fluorescent protein (GFP)-expressing MDA-MB-231 TNBC cells (231s) were purchased from American Type Culture Collection (ATCC) and cultured in Dulbecco's modified Eagle's medium (DMEM; Thermo Fisher) supplemented with 10% (v/v) fetal bovine serum (FBS; Thermo Fisher) and 1% (v/v) penicillin–streptomycin (Lonza), using T25 flasks at 37 °C and 5% CO_2. Experiments used cells between passages 35 and 40. To prepare 231s for co-culture with HMVEC-Ls, the 231s were washed with warm 1× PBS and resuspended in HMVEC-L media at 10,000 cells/mL. Basal or inflamed HMVEC-Ls were treated with NS or left untreated as described above, followed by washing 3× with 1× PBS. One milliliter of the 231 cell solution was incubated with the HMVEC-L samples. After incubating for 4 h at 37 °C and 5% CO_2, samples were washed 5× with pre-warmed 1× PBS to remove any NS and 231s that did not bind to the HMVEC-Ls, fixed with 4% formaldehyde, and rinsed 3× with 1× PBS. After fixation, the chamber walls were removed and the cells counterstained with DAPI in Prolong Gold and stored at 4 °C prior to imaging and analysis. Cells were imaged with the same methods as described above, except that NS were not visualized and instead the 231s were visualized using excitation/emission of 488/509. To quantify bound GFP-MDA-MB-231 cells to HMVEC-Ls, the number of 231s in each image was counted and normalized to the surface area.

RESULTS

Quantifying the Influence of PEG Linker Length on NS Antibody Loading, Hydrodynamic Diameter, and Zeta Potential. Both 2 and 5 kDa OPSS-PEG-SVA were used to non-directionally conjugate antibodies (Abs) to NS to determine which linker length provided the highest antibody loading. These conjugates are referred to as NS-2k-AB and NS-5k-AB for the 2 and 5 kDa molecular weights, respectively. ELISA quantification indicated that the numbers of Abs loaded on the NS were 162 ± 1.4 and 262 ± 30.5 for 2k and 5k linkers, respectively, indicating that the longer linker yielded higher antibody loading (Figure 1A). NS-5k-AB also exhibited a larger hydrodynamic diameter but a similar zeta potential to NS-2k-AB (Figure 1B,C). The hydrodynamic diameter of bare NS was 146 ± 8.8 nm, compared to 163 ± 12.5 nm for NS-PEG and 163 ± 12.1 nm for NS-2k-AB. The NS-5k-AB had a noticeably larger hydrodynamic diameter of 199 ± 2.0 nm, owing to the increased linker length (Figure 1B). The zeta potential of bare NS was −34.5 ± 2.0 mV, which increased over 3× to −10.7 ± 0.1 mV for NS-PEG (Figure 1C). No significant difference was observed between zeta potentials of NS-PEG, NS-2k-AB, or NS-5k-AB, indicating that increased antibody loading had a minimal influence on surface charge.

We also investigated the influence of linker length on Ab loading for the directional conjugation method, using 5 and 10 kDa thiol-PEG-hydrazide. When conjugating via the directional method with a 5 kDa thiol-PEG-hydrazide linker, there was an increased number of Abs on the NS (146 ± 35)

https://doi.org/10.1021/acsanm.2c04967
ACS Appl. Nano Mater. XXXX, XXX, XXX−XXX

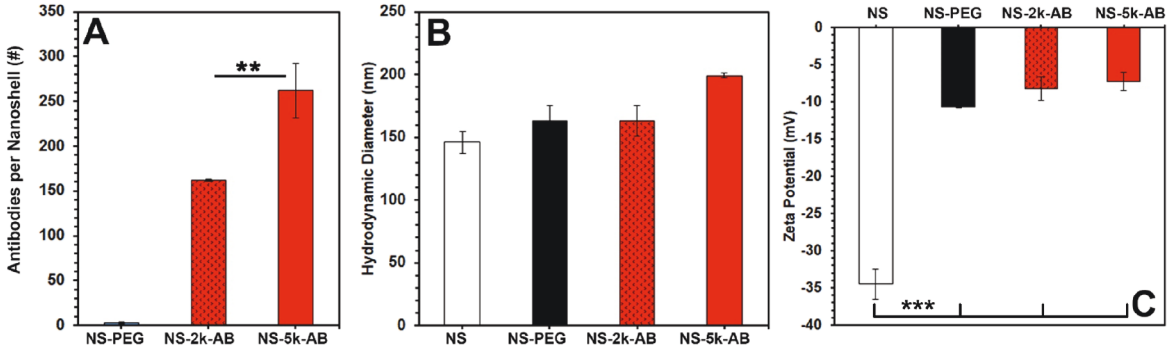

Figure 1. Characterization of NS functionalized with E-selectin antibodies via non-directional conjugation using 2 or 5 kDa OPSS-PEG-SVA linkers. NS-2k-AB and NS-5k-AB indicate NS functionalized with E-selectin antibodies via OPSS-PEG$_{2000}$-SVA or OPSS-PEG$_{5000}$-SVA linkers, respectively, and passivated with 5 kDa mPEG-SH. NS-PEG indicates NS functionalized with only 5 kDa mPEG-SH. Antibodies were added to NS at a 1000:1 (antibody/NS) ratio, and mPEG-SH was added at 10 μM. The functionalized NS were characterized using ELISA assays and DLS measurements to quantify (A) the number of E-selectin antibodies per NS, (B) the hydrodynamic diameter of each conjugate, and (C) the zeta potential of each conjugate. $^{**}p < 0.05$ by Student's t-test. $^{***}p < 0.005$ by one-way ANOVA with post hoc Tukey.

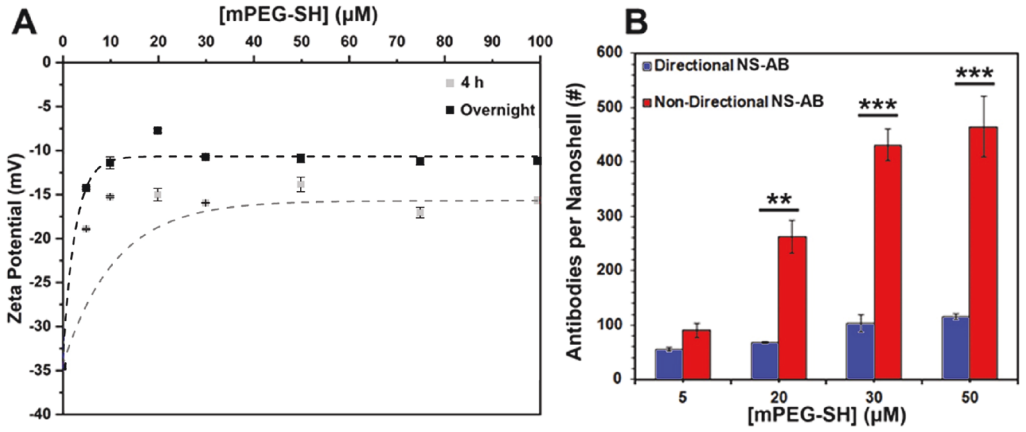

Figure 2. Quantifying the influence of mPEG-SH backfill concentration on NS zeta potential and antibody loading capacity. (A) Zeta potential measurements of NS incubated with increasing concentrations of 5 kDa mPEG-SH for either 4 h (gray) or overnight (black). (B) Quantification of the number of E-selectin antibodies bound per NS as a function of mPEG-SH concentration following overnight mPEG-SH incubation as determined by ELISA. Antibodies were attached to the NS non-directionally (red) using OPSS-PEG$_{5000}$-SVA linkers or directionally (blue) using SH-PEG$_{5000}$-hydrazide linkers. Both conjugation techniques were performed using an antibody/NS ratio of 1000:1. $^{**}p < 0.05$ and $^{***}p < 0.005$ by Student's t-test.

compared to conjugation with the 10 kDa linker (25 ± 15) (Figure S2). We postulate that this counterintuitive result may be due to steric hindrance or charge interactions between neighboring Abs or due to less efficient conjugation of the Abs with the 10 kDa thiol-PEG-hydrazide than with the 5 kDa thiol-PEG-hydrazide.

Quantifying the Influence of mPEG-SH Concentration on NS Zeta Potential and Antibody Loading. To quantify the influence of mPEG-SH concentration [PEG] on NS zeta potential and antibody loading, we prepared NS-AB as described above, with the concentration of 5 kDa mPEG-SH varied from 5 to 100 μM. For these experiments, 5 kDa OPSS-PEG-SVA or thiol-PEG-hydrazide linkers were used for E-selectin Ab loading. As mPEG-SH neutralizes the surface charge, the NS were considered fully passivated when addition of more mPEG-SH did not yield a further increase in zeta potential. This analysis indicated that the surface of NS was saturated with mPEG-SH at a concentration of 30 μM (Figure 2A). We also examined the influence of incubation time and determined that overnight incubation of mPEG-SH neutralized the NS surface more than 4 h incubation but that reaction time had less influence than concentration. Plotting the zeta potential against [PEG] reveals a logarithmic trend for both incubation times (Figure 2A).

The influence of mPEG-SH concentration on antibody loading for NS prepared by both directional and non-directional conjugation methods was also investigated. The ratio of Ab added was maintained at 1000 Ab/1 NS, while the concentration of mPEG-SH ranged from 5 to 50 μM with the samples incubated overnight at 4 °C prior to purification and antibody loading analysis by ELISA. Increasing [PEG] from 5 to 30 μM led to increased Ab loading, and loading was saturated for [PEG] beyond ~30 μM (Figure 2B). Increasing the concentration of mPEG-SH up to 30 μM elevated Ab loading by 4.8× and 1.8× for the non-directional and directional conjugation methods, respectively. Beyond that, modest changes of ~7% for non-directional and ~10% for directional conjugation were observed (Figure 2B). We postulate that the positive correlation between Ab loading and mPEG-SH concentration is due to higher densities of mPEG-SH on the NS surface forcing the PEGylated Abs to orient radially, rather than folding back onto the NS surface.

We found that Ab loading was noticeably lower for NS prepared by directional conjugation versus non-directional

https://doi.org/10.1021/acsanm.2c04967
ACS Appl. Nano Mater. XXXX, XXX, XXX−XXX

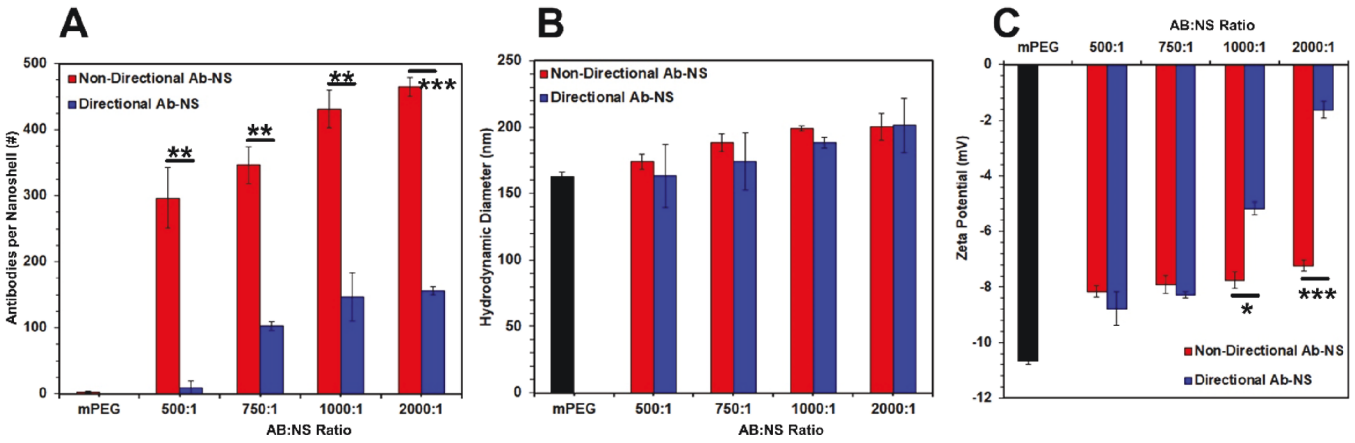

Figure 3. Characterization of E-selectin antibody-functionalized NS prepared by non-directional or directional functionalization at AB/NS ratios ranging from 500:1 to 2000:1. Quantification of the (A) number of E-selectin antibodies bound per NS as determined by ELISA, (B) hydrodynamic diameter of NS-AB as determined by DLS, and (C) zeta potential of NS-AB. NS-PEG indicates NS functionalized with only 5 kDa mPEG-SH. Non-directional NS-AB (red) and directional NS-AB (blue) were functionalized with E-selectin antibodies using non-directional or directional conjugation at incubation ratios of 500:1, 750:1, 1000:1, or 2000:1 (AB/NS), followed by overnight passivation with 30 μM 5 kDa mPEG-SH. *p < 0.1, **p < 0.05, and ***p < 0.005 by Student's t-test.

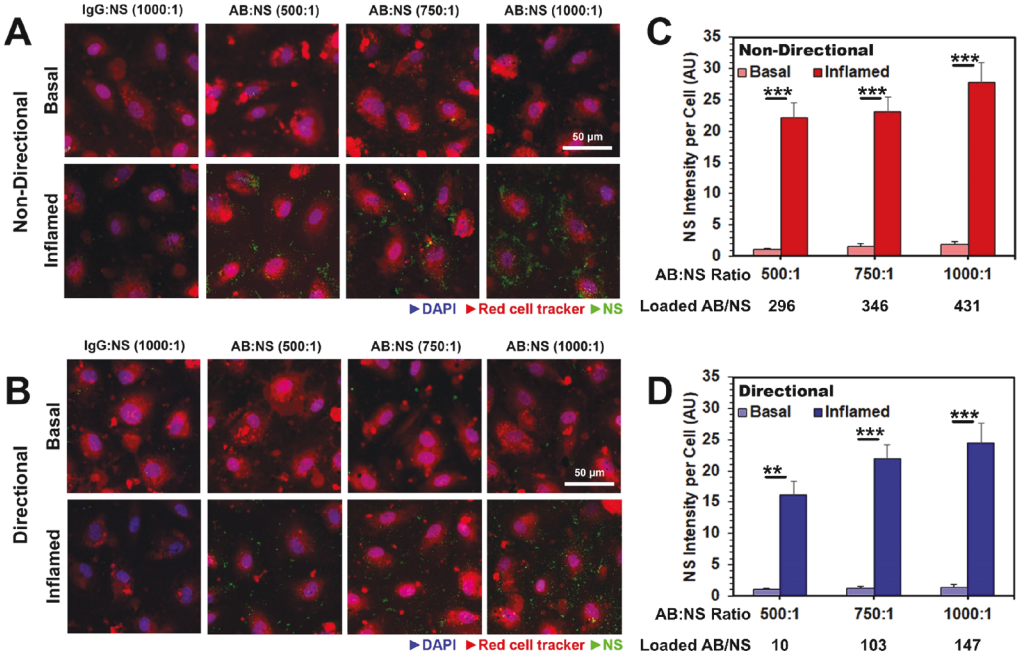

Figure 4. Characterization of E-selectin NS-AB binding to basal and inflamed ECs. (A, B) Two-photon photoluminescence images of (A) non-directionally or (B) directionally functionalized NS-AB bound to HMVEC-Ls in basal or inflamed conditions. Control IgG-NS were prepared at a 1000:1 AB/NS ratio, while E-selectin NS-AB were prepared and evaluated at 500:1, 750:1, and 1000:1 AB/NS ratios. Blue = nuclei (DAPI), red = cell tracker, green = NS (two-photon photoluminescence). (C, D) Quantification of NS intensity per cell based on image intensity measurements. **p < 0.05 and ***p < 0.005 by Student's t-test. AB means E-selectin.

conjugation across all mPEG-SH concentrations tested (Figure 2B). This may be because of the antibody orientation. In the directional method, the Fab region of the antibodies is oriented outward.[29] With antibodies stacking next to each other as they bind the NS surface, the specific orientation may create steric hindrance in which only a limited amount of Abs can physically fit next to each other on the NS surface. Using the non-directional method, the antibody orientation is random, which allows the antibodies to pack more densely by taking on more favorable positions, owing to linker flexibility and folding.

The quantitative ELISA results demonstrating increased Ab loading for NS prepared using non-directional conjugation were corroborated by the relative magnitude of the shift in the NS peak extinction for samples prepared by non-directional versus directional conjugation using 1000:1 Abs/NS, 5 kDa linkers, and 30 μM mPEG-SH (Figure S3). Bare NS exhibit a characteristic dipole resonance peak at ~800 nm and a quadrupole resonance at ~600 nm, and these peaks red-shift after NS are coated with biomolecules. For the specific batch shown in Figure S3, the peak resonance wavelength was ~776 nm for bare NS, ~786 nm for directional NS-AB, and ~792 nm for non-directional NS-AB.

https://doi.org/10.1021/acsanm.2c04967
ACS Appl. Nano Mater. XXXX, XXX, XXX−XXX

Quantifying the Influence of the AB/NS Incubation Ratio on Antibody Loading. The number of Abs loaded on NS was also quantified as a function of the ratio of Abs to NS, with the AB/NS incubation ratio adjusted from 500:1 to 2000:1 while maintaining a constant mPEG-SH backfill concentration of 30 μM. For both directional and non-directional conjugation methods, Ab loading positively correlated with the amount of Ab incubated for the interval of 500:1 to 1000:1 Ab to NS (Figure 3A). This correlation was not retained with the AB/NS incubation ratio to 2000:1, as the Ab loading became saturated. Consistent with the results presented in Figure 2, non-directional conjugation yielded higher Ab loading than directional conjugation across all ratios evaluated. Specifically, NS-AB prepared using non-directional conjugation had 30, 3.3, 2.9, and 3.0 times more Abs loaded than NS-AB prepared using directional conjugation when the AB/NS incubation ratio was 500, 750, 1000, and 2000, respectively. The hydrodynamic diameter and zeta potential of NS-AB for each method were also measured (Figure 3B,C). At any given AB/NS incubation ratio, there was no significant difference in the hydrodynamic diameter of NS-AB prepared by directional or non-directional conjugation, but the hydrodynamic diameter of each conjugate did increase slightly as the AB/NS incubation ratio increased (Figure 3B). Similarly, zeta potentials became more neutral as the AB/NS incubation ratio increased (Figure 3C). There was no difference in zeta potential between directional and non-directional conjugation for incubation ratios below 750:1, but directional NS-AB were significantly more neutral than non-directional NS-AB at incubation ratios above 1000:1. Based on the combined results of the characterization, we chose to prepare E-selectin antibody-conjugated NS for subsequent experiments using an AB/NS incubation ratio of 1000:1 and overnight incubation with mPEG-SH at 30 μM. We also evaluated the ability to store NS-AB for up to 30 days at either 4 or −20 °C and determined via ELISA that storage under these conditions did not significantly impact Ab loading (Figure S4).

Binding of Non-Directional and Directional E-Selectin NS to Inflamed HMVEC-Ls. Experiments were performed to determine if antibody loading density impacted E-selectin NS binding to HMVEC-Ls. Both non-directional and directional E-selectin NS binding was quantified by imaging NS bound to ECs using two-photon microscopy and measuring the NS photoluminescence intensity for each condition. Figure 4A,B displays merged images of the cells (CytoTracker Red), their nuclei (DAPI, blue), and the NS two-photon-induced photoluminescence (TPL) signal (green). Since HMVEC-Ls express low levels of E-selectin in the basal, non-inflamed culture condition, they were stimulated with 10 ng/mL TNF-α for 6 h to increase E-selectin expression, as experiments showed that this exposure time yields maximum E-selectin expression (Figure S5). As expected, both directional and non-directional E-selectin-targeted NS exhibited greater binding to inflamed HMVEC-Ls than basal (non-inflamed) ECs (Figure 4). The TPL signal from the NS was quantified to provide a measure of relative binding to basal or inflamed ECs as a function of antibody loading density (Figure 4C,D). This showed that (i) increased Ab loading yielded increased binding to HMVEC-Ls for both non-directional (Figure 4C) and directional (Figure 4D) NS-AB formulations and (ii) despite having lower antibody loading, NS functionalized with the directional method bound inflamed HMVEC-Ls nearly as well as NS functionalized with the non-directional method (Figure 4C,D).

To determine if the observed HMVEC-L binding could be attributed to the E-selectin antibodies on the NS, these experiments were also performed using NS coated with anti-mouse IgG nonspecific antibodies as a control (Figure 4A,B). These NPs were marginally detected; this result, combined with the increased binding of E-selectin NS to inflamed versus basal HMVEC-Ls, indicated that the observed binding was primarily due to the E-selectin antibodies present on the NS.

Inhibiting Cancer Cell Docking to Inflamed ECs with E-Selectin-Functionalized NS. After confirming successful binding of E-selectin-functionalized NS to HMVEC-Ls, we evaluated whether NS binding could reduce MDA-MB-231 docking. If so, this would provide proof of concept that antibody-functionalized NS may be able to inhibit CTC binding to the lung endothelium (although this would need to be validated using more complex models in future work). Fluorescence confocal microscopy was used to visualize GFP-expressing MDA-MB-231 cell binding to basal HMVEC-Ls or those that were treated with TNF-α to induce inflammation and exposed to either no treatment or E-selectin NS-AB prepared by non-directional conjugation at an AB/NS ratio of 1000:1 (Figure 5A). Samples were treated with NS-AB at concentrations of OD^{800nm} = 2.5 (~6.8 × 10^9 NS/mL), OD^{800nm} = 5 (~1.4 × 10^{10} NS/mL), or OD^{800nm} = 7.5 (~2.1 × 10^{10} NS/mL) (Figure S6). Images were analyzed to reveal the density of 231s (# of cells per mm^2) bound to basal or inflamed HMVEC-Ls in each condition (Figure 5B). Owing to elevated E-selectin expression, GFP-231s exhibited more binding to HMVEC-Ls in the inflamed condition versus the basal, non-inflamed control (Figure 5 and Figure S6). However, the number of bound 231s dropped significantly when HMVEC-Ls were pre-treated with NS-AB (Figure 5 and Figure S6), with more pronounced effects observed for inflamed samples than for basal samples. While increasing NS-AB concentration from OD^{800nm} = 2.5 to OD^{800nm} = 5 had a noteworthy impact on 231 binding to ECs, further increasing the concentration to OD^{800nm} = 7.5 did not increase inhibition (Figure 5B and Figure S6). This suggests that the binding sites for NS-AB and GFP-231s were saturated, and maximum effects had been achieved under the conditions tested here.

DISCUSSION

The ability to inhibit CTC binding to, and extravasation through, the endothelium has potential to reduce metastatic burden in cancer patients.[30,31] Several strategies can be implemented to inhibit CTC binding to ECs including (i) reducing expression of EC-expressed CAMs using anti-inflammatory compounds,[30−33] (ii) targeting and blocking receptors on CTCs with antibodies to inhibit interactions with ECs,[34,35] or (iii) targeting and blocking CAMs, expressed by ECs, with antibodies to inhibit interactions with CTCs.[34−36] All three of these approaches have shown promise in inhibiting CTC docking to ECs. Here, we implemented antibody targeting of EC-expressed E-selectin using antibody-functionalized NPs. Compared to free antibodies, antibody−NP conjugates exhibit multivalent binding to targeted receptors, which increases avidity and efficacy,[24,37] and are therefore used in this study.

We characterized and compared two conjugation methods, directional and non-directional, to prepare E-selectin antibody-functionalized NS and evaluated their ability to bind basal and

https://doi.org/10.1021/acsanm.2c04967
ACS Appl. Nano Mater. XXXX, XXX, XXX−XXX

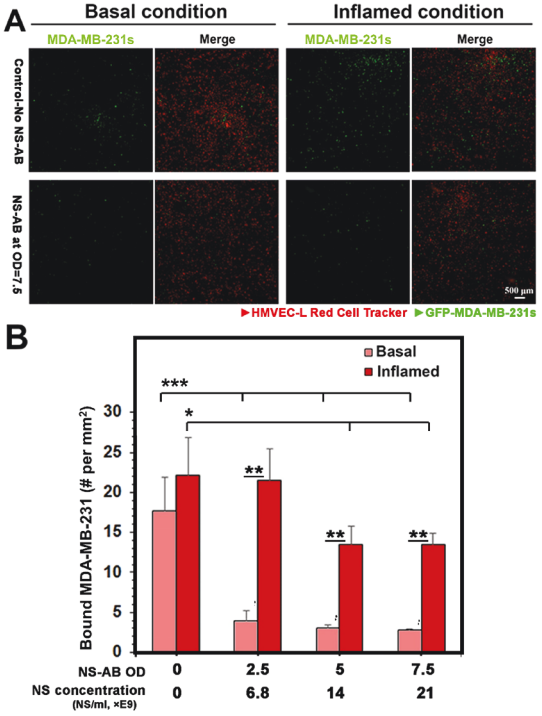

Figure 5. Inhibition of MDA-MB-231 binding to HMVEC-Ls using E-selectin antibody-functionalized NS. (A) Fluorescence images showing GFP-MDA-MB-231 cells bound to HMVEC-Ls treated with or without E-selectin antibody-functionalized NS at OD^{800nm} = 7.5 (corresponding to 21 × 10^9 NS/mL) in basal or inflamed conditions. Red = HMVEC-L red cell tracker, green = GFP-MDA-MB-231 cells. (B) Quantification of GFP-MDA-MB-231 binding (# of cells per mm^2) to basal or inflamed HMVEC-Ls that were pretreated with E-selectin NS-AB at concentrations of OD^{800nm} = 0, 2.5, 5, or 7.5 based on fluorescent images (representative images shown in Figure S6). *p < 0.05 for inflamed condition at NS OD = 5 and OD = 7.5 versus OD = 0 by one-way ANOVA, **p < 0.01 for basal versus inflamed condition at each NS OD by Student's t-test, and ***p < 0.001 for basal condition at NS OD = 2.5, OD = 5, and OD = 7.5 versus OD = 0 by one-way ANOVA.

inflamed lung ECs and subsequently inhibit MDA-MB-231 cell docking. The results demonstrate that the number of Abs conjugated to the NS depends on the conjugation method employed. The non-directional method yields higher Ab loading compared to the directional approach (Figures 2 and 3), which we attribute to the ability of Abs on non-directional NS to orient in a manner that will maximize loading density, whereas Abs on directional NS are subject to more steric hindrance. Other parameters, including PEG linker length (Figure 1), mPEG-SH concentration (Figure 2), and the ratio of AB/NS utilized during functionalization (Figure 3), also influenced Ab loading. It is important to understand the influence of each parameter, as our studies demonstrate that Ab loading influences the NS ability to bind HMVEC-Ls (Figure 4). Specifically, NS coated with more Abs exhibit increased EC binding, particularly under inflamed conditions when E-selectin is overexpressed by HMVEC-Ls. Our studies also exploited NS photoluminescent properties to evaluate their cellular binding. As two-photon microscopy is amenable to *in vivo* use since it can provide subcellular resolution at depths of up to several hundred microns in tissue,[38] one could envision utilizing this approach in the future to confirm NS-AB delivery to the desired sites of inflammation *in vivo*.

Linker length is an important parameter to consider when designing NS-AB conjugates for cell targeting. If the PEG chains used to link NS with Abs are shorter than the passivating mPEG-SH (e.g., 2 versus 5 kDa), the functional head of the Ab may be hidden from the surrounding environment, which can limit the ability to bind targeted receptors on cell surfaces.[39] If the PEG linker is longer than the passivating mPEG-SH (e.g., 10 versus 5 kDa), the Abs could fold back onto the NS surface, even using the directional method, reducing loading density by preventing other molecules from reaching the NS surface.[39] Indeed, we found that NS-AB prepared by directional conjugation with 10 kDa PEG linkers had substantially reduced loading compared to NS-AB prepared with 5 kDa linkers. These results suggest that the Ab loading density is maximized on NS when the length of the PEG linker is similar to that of the mPEG passivating agent.

We also found that mPEG-SH concentration was important for controlling both Ab loading on NS and the zeta potential of the resultant NS-AB. Under the conditions tested here, 30 μM mPEG-SH was sufficient to neutralize the zeta potential of the NPs and maximize Ab loading (Figure 2). Given that mPEG-SH decreases nonspecific protein adsorption and clearance of NPs by the mononuclear phagocytic system, it is important to synthesize NS-AB conjugates under conditions that yield maximal "shielding", as this will translate to extended circulation time and improved performance *in vivo*.

Our studies revealed differences between NS-AB prepared by non-directional and directional methods when evaluating the binding to HMVEC-Ls *in vitro*. Despite having significantly less antibody loading, directionally conjugated NS-AB were able to bind inflamed ECs almost as well as non-directionally conjugated NS-AB (Figure 4). This is likely due to the orientation of the antibodies. With the directional method, the Fab regions are exposed, while they may be hidden with the non-directional method. Accordingly, non-directional NS-AB with greater overall Ab loading exhibited similar (although slightly lower) levels of binding to ECs compared to directionally functionalized NS-AB with lower overall Ab loading. Given the relative simplicity and lower cost of the non-directional method, coupled with the greater binding to HMVEC-Ls, NS-ABs prepared with this conjugation technique were selected for further analysis regarding the ability to inhibit MDA-MB-231s from binding lung microvascular ECs. We found that E-selectin NS-AB conjugates could reduce MDA-MB-231 binding to inflamed HMVEC-Ls by 36% at NS-AB concentrations of 1.4 × 10^{10} NS/mL and by 41% at 2.1 × 10^{10} NS/mL (Figure 5). This provides proof of concept that NS targeting E-selectin could block CTC binding to the endothelium. This remains to be validated in more complex *in vitro* models that incorporate fluid flow and the ability to quantify extravasation rates as well as in animal models. While 41% inhibition is significant, we anticipate that higher efficacy could be achieved using NS functionalized with additional antibodies against CAMs implicated in CTC binding to ECs—VCAM1 and ICAM1, for example.

■ CONCLUSIONS

Overall, this study provides important insight to the design parameters that can be controlled to tailor the production of Ab-coated NS and for the use of E-selectin-targeted NS for possible prevention of CTC binding to the lung microvascular endothelium. Future studies that build on this work will

https://doi.org/10.1021/acsanm.2c04967
ACS Appl. Nano Mater. XXXX, XXX, XXX−XXX

evaluate the approach in more dynamic conditions that mimic *in vivo* scenarios toward the goal of providing a strategy to limit CTC extravasation that leads to metastasis.

■ ASSOCIATED CONTENT

Supporting Information

The Supporting Information is available free of charge at https://pubs.acs.org/doi/10.1021/acsanm.2c04967.

TEM of bare NS; antibodies per NS; extinction spectra; stability after 1 month storage; E-selectin expression by ECs; and 231 binding to treated ECs (PDF)

■ AUTHOR INFORMATION

Corresponding Author

J.H. Slater − *Department of Biomedical Engineering, University of Delaware, Newark, Delaware 19713, United States;* orcid.org/0000-0002-2453-6665; Email: jhslater@udel.edu

Authors

Z. Fereshteh − *Department of Biomedical Engineering, University of Delaware, Newark, Delaware 19713, United States*

M.N. Dang − *Department of Biomedical Engineering, University of Delaware, Newark, Delaware 19713, United States;* orcid.org/0000-0002-4222-3355

C. Wenck − *Department of Biomedical Engineering, University of Delaware, Newark, Delaware 19713, United States*

E.S. Day − *Department of Biomedical Engineering, University of Delaware, Newark, Delaware 19713, United States;* orcid.org/0000-0002-8707-826X

Complete contact information is available at: https://pubs.acs.org/10.1021/acsanm.2c04967

Funding

This work was supported by the National Institutes of Health (NIH) under grant numbers R01CA211925 (ESD), R35GM119659 (ESD), T32GM133395 (MND), and P20GM113125 (JHS) and the National Science Foundation 1751797 (JHS). Microscopy access was supported by grants from the NIH (P20GM103446), the National Science Foundation (IIA-1301765), and the State of Delaware. The content is solely the responsibility of the authors and does not necessarily reflect the views of the funding agencies.

Notes

The authors declare no competing financial interest.

■ REFERENCES

(1) Rejniak, K. A. Circulating Tumor Cells: When a Solid Tumor Meets a Fluid Microenvironment. *Adv. Exp. Med. Biol.* **2016**, *936*, 93−106.

(2) Shenoy, A. K.; Lu, J. Cancer Cells Remodel Themselves and Vasculature to Overcome the Endothelial Barrier. *Cancer Lett.* **2016**, *380*, 534−544.

(3) Sökeland, G.; Schumacher, U. The Functional Role of Integrins During Intra- and Extravasation within the Metastatic Cascade. *Mol. Cancer* **2019**, *18*, 12.

(4) Dittmar, T.; Heyder, C.; Gloria-Maercker, E.; Hatzmann, W.; Zänker, K. S. Adhesion Molecules and Chemokines: The Navigation System for Circulating Tumor (Stem) Cells to Metastasize in an Organ-Specific Manner. *Clin. Exp. Metastasis* **2008**, *25*, 11−32.

(5) Makrilia, N.; Kollias, A.; Manolopoulos, L.; Syrigos, K. Cell Adhesion Molecules: Role and Clinical Significance in Cancer. *Cancer Invest.* **2009**, *27*, 1023−1037.

(6) Balzer, E. M.; Konstantopoulos, K. Intercellular Adhesion: Mechanisms for Growth and Metastasis of Epithelial Cancers. *Wiley Interdiscip. Rev.: Syst. Biol. Med.* **2012**, *4*, 171−181.

(7) Li, D. M.; Feng, Y. M. Signaling Mechanism of Cell Adhesion Molecules in Breast Cancer Metastasis: Potential Therapeutic Targets. *Breast Cancer Res. Treat.* **2011**, *128*, 7−21.

(8) Stewart, B. W.; Wild, C. P., *World Cancer Report 2014.*; World Health Organization. 2014.

(9) Liedtke, C.; Mazouni, C.; Hess, K. R.; André, F.; Tordai, A.; Mejia, J. A.; Symmans, W. F.; Gonzalez-Angulo, A. M.; Hennessy, B.; Green, M.; Cristofanilli, M.; Hortobagyi, G. N.; Pusztai, L. Response to Neoadjuvant Therapy and Long-Term Survival in Patients with Triple-Negative Breast Cancer. *J. Clin. Oncol.* **2008**, *26*, 1275−1281.

(10) Kuo, W. H.; Chang, Y. Y.; Lai, L. C.; Tsai, M. H.; Hsiao, C. K.; Chang, K. J.; Chuang, E. Y. Molecular Characteristics and Metastasis Predictor Genes of Triple-Negative Breast Cancer: A Clinical Study of Triple-Negative Breast Carcinomas. *PLoS One* **2012**, *7*, No. e45831.

(11) Bianchini, G.; Balko, J. M.; Mayer, I. A.; Sanders, M. E.; Gianni, L. Triple-Negative Breast Cancer: Challenges and Opportunities of a Heterogeneous Disease. *Nat. Rev. Clin. Oncol.* **2016**, *13*, 674−690.

(12) DeSantis, C. E.; Ma, J.; Gaudet, M. M.; Newman, L. A.; Miller, K. D.; Goding Sauer, A.; Jemal, A.; Siegel, R. L. Breast Cancer Statistics, 2019. *Ca-Cancer J. Clin.* **2019**, *69*, 438−451.

(13) Dent, R.; Hanna, W. M.; Trudeau, M.; Rawlinson, E.; Sun, P.; Narod, S. A. Pattern of Metastatic Spread in Triple-Negative Breast Cancer. *Breast Cancer Res. Treat.* **2009**, *115*, 423−428.

(14) Barthel, S. R.; Gavino, J. D.; Descheny, L.; Dimitroff, C. J. Targeting Selectins and Selectin Ligands in Inflammation and Cancer. *Expert Opin. Ther. Targets* **2007**, *11*, 1473−1491.

(15) Roche, W. R.; Montefort, S.; Baker, J.; Holgate, S. T. Cell Adhesion Molecules and the Bronchial Epithelium. *Am. Rev. Respir. Dis.* **1993**, *148*, S79−S82.

(16) Gad, S. C.; Sharp, K. L.; Montgomery, C.; Payne, J. D.; Goodrich, G. P. Evaluation of the Toxicity of Intravenous Delivery of Auroshell Particles (Gold-Silica Nanoshells). *Int. J. Toxicol.* **2012**, *31*, 584−594.

(17) Stern, J. M.; Kibanov Solomonov, V. V.; Sazykina, E.; Schwartz, J. A.; Gad, S. C.; Goodrich, G. P. Initial Evaluation of the Safety of Nanoshell-Directed Photothermal Therapy in the Treatment of Prostate Disease. *Int. J. Toxicol.* **2016**, *35*, 38−46.

(18) Rastinehad, A. R.; Anastos, H.; Wajswol, E.; Winoker, J. S.; Sfakianos, J. P.; Doppalapudi, S. K.; Carrick, M. R.; Knauer, C. J.; Taouli, B.; Lewis, S. C.; Tewari, A. K.; Schwartz, J. A.; Canfield, S. E.; George, A. K.; West, J. L.; Halas, N. J. Gold Nanoshell-Localized Photothermal Ablation of Prostate Tumors in a Clinical Pilot Device Study. *Proc. Natl. Acad. Sci. U. S. A.* **2019**, *116*, 18590−18596.

(19) Day, E. S.; Bickford, L. R.; Slater, J. H.; Riggall, N. S.; Drezek, R. A.; West, J. L. Antibody-Conjugated Gold-Gold Sulfide Nanoparticles as Multifunctional Agents for Imaging and Therapy of Breast Cancer. *Int. J. Nanomed.* **2010**, *5*, 445−454.

(20) Gao, L.; Vadakkan, T. J.; Nammalvar, V. Nanoshells for in Vivo Imaging Using Two-Photon Excitation Microscopy. *Nanotechnology* **2011**, *22*, No. 365102.

(21) Coughlin, A. J.; Ananta, J. S.; Deng, N.; Larina, I. V.; Decuzzi, P.; West, J. L. Gadolinium-Conjugated Gold Nanoshells for Multimodal Diagnostic Imaging and Photothermal Cancer Therapy. *Small* **2014**, *10*, 556−565.

(22) Gao, X.; Kan, B.; Gou, M.; Zhang, J.; Guo, G.; Huang, N.; Zhao, X.; Qian, Z. Preparation of Anti-Cd40 Antibody Modified Magnetic Pcl-Peg-Pcl Microspheres. *J. Biomed. Nanotechnol.* **2011**, *7*, 285−291.

(23) Park, J.; Estrada, A.; Sharp, K.; Sang, K.; Schwartz, J. A.; Smith, D. K.; Coleman, C.; Payne, J. D.; Korgel, B. A.; Dunn, A. K.; Tunnell, J. W. Two-Photon-Induced Photoluminescence Imaging of Tumors Using near-Infrared Excited Gold Nanoshells. *Opt. Express* **2008**, *16*, 1590−1599.

(24) Dang, M. N.; Hoover, E. C.; Scully, M. A.; Sterin, E. H.; Day, E. S. Antibody Nanocarriers for Cancer Management. *Curr. Opin. Biomed. Eng.* **2021**, *19*, No. 100295.
(25) Kumar, S.; Aaron, J.; Sokolov, K. Directional Conjugation of Antibodies to Nanoparticles for Synthesis of Multiplexed Optical Contrast Agents with Both Delivery and Targeting Moieties. *Nat. Protoc.* **2008**, *3*, 314−320.
(26) Oldenburg, S. J.; Averitt, R. D.; Westcott, S. L.; Halas, N. J. Nanoengineering of Optical Resonances. *Chem. Phys. Lett.* **1998**, *288*, 243−247.
(27) Lowery, A. R.; Gobin, A. M.; Day, E. S.; Halas, N. J.; West, J. L. Immunonanoshells for Targeted Photothermal Ablation of Tumor Cells. *Int. J. Nanomed.* **2006**, *1*, 149−154.
(28) Riley, R. S.; Melamed, J. R.; Day, E. S., Enzyme-Linked Immunosorbent Assay to Quantify Targeting Molecules on Nanoparticles. In *Targeted Drug Delivery: Methods and Protocols*, Sirianni, R. W.; Behkam, B., Eds. Springer US: New York, NY, 2018, pp. 145−157, DOI: 10.1007/978-1-4939-8661-3_11.
(29) Zhou, S.; Hu, J.; Chen, X.; Duan, H.; Shao, Y.; Lin, T.; Li, X.; Huang, X.; Xiong, Y. Hydrazide-Assisted Directional Antibody Conjugation of Gold Nanoparticles to Enhance Immunochromatographic Assay. *Anal. Chim. Acta* **2021**, *1168*, No. 338623.
(30) Nojiri, T.; Hosoda, H.; Tokudome, T.; Miura, K.; Ishikane, S.; Otani, K.; Kishimoto, I.; Shintani, Y.; Inoue, M.; Kimura, T.; Sawabata, N.; Minami, M.; Nakagiri, T.; Funaki, S.; Takeuchi, Y.; Maeda, H.; Kidoya, H.; Kiyonari, H.; Shioi, G.; Arai, Y.; Hasegawa, T.; Takakura, N.; Hori, M.; Ohno, Y.; Miyazato, M.; Mochizuki, N.; Okumura, M.; Kangawa, K. Atrial Natriuretic Peptide Prevents Cancer Metastasis through Vascular Endothelial Cells. *Proc. Natl. Acad. Sci. U. S. A.* **2015**, *112*, 4086−4091.
(31) Hanako, K.; Kimberly, C. B.; Lin, P. C. Endothelial Cell Adhesion Molecules and Cancer Progression. *Curr. Med. Chem.* **2007**, *14*, 377−386.
(32) Kobayashi, K.; Matsumoto, S.; Morishima, T.; Kawabe, T.; Okamoto, T. Cimetidine Inhibits Cancer Cell Adhesion to Endothelial Cells and Prevents Metastasis by Blocking E-Selectin Expression. *Cancer Res.* **2000**, *60*, 3978−3984.
(33) Tozawa, K.; Kawai, N.; Hayashi, Y.; Sasaki, S.; Kohri, K.; Okamoto, T. Gold Compounds Inhibit Adhesion of Human Cancer Cells to Vascular Endothelial Cells. *Cancer Lett.* **2003**, *196*, 93−100.
(34) Mattila, P.; Majuri, M.-L.; Renkonen, R. Vla-4 Integrin on Sarcoma Cell Lines Recognizes Endothelial Vcam-1. Differential Regulation of the Vla-4 Avidity on Various Sarcoma Cell Lines. *Int. J. Cancer* **1992**, *52*, 918−923.
(35) Dong, C.; Slattery, M. J.; Liang, S.; Peng, H. H. Melanoma Cell Extravasation under Flow Conditions Is Modulated by Leukocytes and Endogenously Produced Interleukin 8. *Mol. Cell. Biol.* **2005**, *2*, 145−159.
(36) Okada, T.; Hawley, R. G.; Kodaka, M.; Okuno, H. Significance of Vla-4−Vcam-1 Interaction and Cd44 for Transendothelial Invasion in a Bone Marrow Metastatic Myeloma Model. *Clin. Exp. Metastasis* **1999**, *17*, 623−629.
(37) Riley, R. S.; Day, E. S. Frizzled7 Antibody-Functionalized Nanoshells Enable Multivalent Binding for Wnt Signaling Inhibition in Triple Negative Breast Cancer Cells. *Small* **2017**, *13*, No. 1700544.
(38) Zipfel, W. R.; Williams, R. M.; Webb, W. W. Nonlinear Magic: Multiphoton Microscopy in the Biosciences. *Nat. Biotechnol.* **2003**, *21*, 1369−1377.
(39) Chen, C. C.; Borden, M. A. Ligand Conjugation to Bimodal Poly(Ethylene Glycol) Brush Layers on Microbubbles. *Langmuir* **2010**, *26*, 13183−13194.

https://doi.org/10.1021/acsanm.2c04967
ACS Appl. Nano Mater. XXXX, XXX, XXX−XXX

Supporting Information

E-Selectin Targeted Gold Nanoshells to Inhibit Breast Cancer Cell Binding to Lung Endothelial Cells

Zeinab Fereshteh, Megan N. Dang, Christina Wenck, Emily S. Day, John H. Slater*

Z. Fereshteh, M.N. Dang, C. Wenck, E.S. Day, J.H. Slater
University of Delaware, Department of Biomedical Engineering, 590 Avenue 1743, Newark, DE 19713
E-mail: jhslater@udel.edu

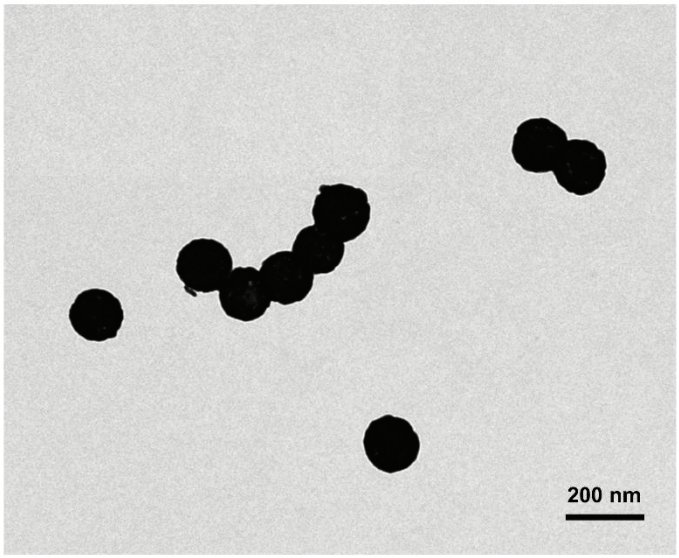

Figure S1. TEM of Bare Nanoshells.

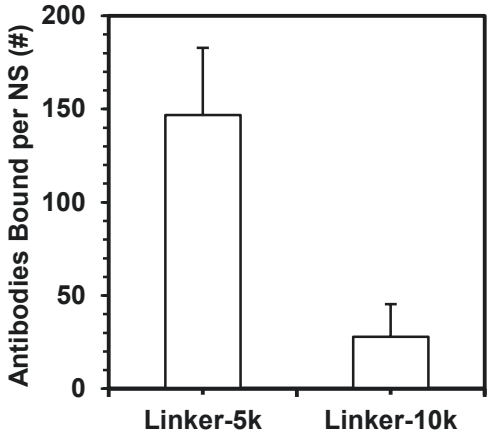

Figure S2. **Characterization of the Number of Antibodies per Nanoshell when Functionalized with E-selectin Antibodies by Directional Conjugation Using 5 kDa or 10 kDa Thiol-PEG-Hydrazide Linkers.** ELISA results show that the number of loaded ABs per NS was significantly higher ($p < 0.05$) for samples prepared with 5 kDa rather than 10 kDa thiol-PEG-Hydrazide.

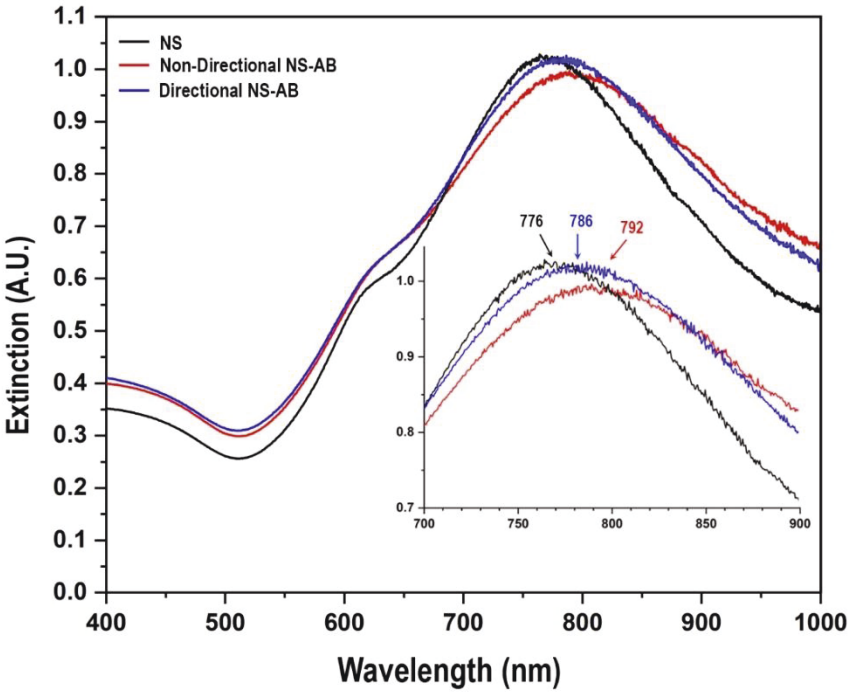

Figure S3. UV-Vis Extinction Spectra of E-Selectin Antibody-Functionalized Nanoshells. Bare, non-functionalized nanoshells (NS, black) displayed a peak plasmon resonance at 776 nm. N231on-directional NS-AB (red) and directional NS-AB (blue) conjugates prepared with a 1000:1 ratio of E-selectin antibodies per NS and passivated with 30 μM mPEG-SH overnight had red-shifted peaks at 792 nm and 786 nm respectively.

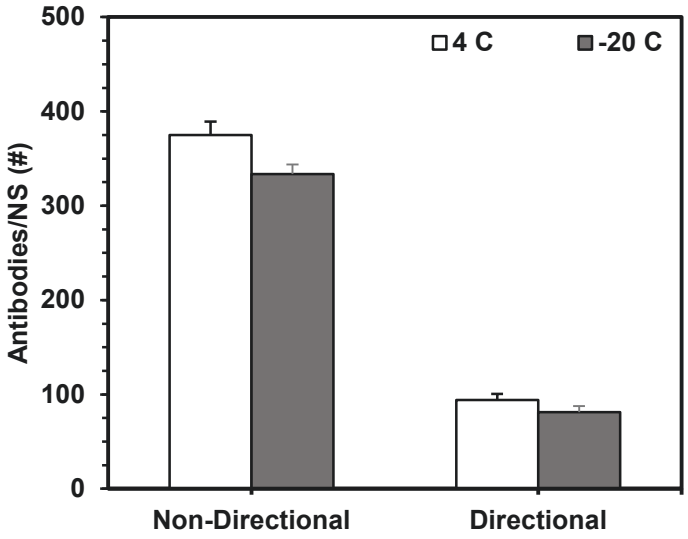

Figure S4. Characterization of E-Selectin Antibody-Functionalized NS after 1 Month of Storage at 4°C or -20°C. Storage temperature for 1 month did not significantly reduce the number of antibodies per nanoshell based on ELISA results. For comparison, freshly prepared directional NS-AB had a loading of 147 ± 35 Ab/NS and non-directional NS-AB had a loading of 431 ± 29 Ab/NS.

Characterization of E-selectin Expression by Inflamed HMVEC-Ls

Non-pooled Human Lung Microvascular Endothelial Cells (HMVEC-Ls) (CC-2527, Group Ltd., Basel, Switzerland) were cultured in tissue-culture flasks in EGM-2MV BulletKit medium (CC-3156 & CC-4147, Group Ltd., Basel, Switzerland) at 37°C and 5% CO_2. Cells were passaged between flasks when they reached 90% confluence by adding 3.0 ml of 0.25% trypsin at 37°C for 3 min. The detached cells were collected, centrifuged to remove excess trypsin, suspended in EGM-2MV (Lonza, CAT # CC-3202), and seeded into culture flasks. All flasks and chamber slides were coated with 10 μg/ml fibronectin from human plasma (FN, F2006, St. Louis, MO, USA) prior to cell seeding. HMVEC-Ls were stimulated with 500 μl of tumor necrosis factor alpha (10 ng/ml TNF-α, 10602-HNAE, Sino Biological Inc., PA, USA) for 4, 6, 8, 12, or 24 hours at 37°C. The cells were washed 3X with pre-warm 1x PBS, fixed with 4%

paraformaldehyde, and rinsed 3X with 1x PBS. After fixation, the cells were labeled with a mouse anti-human E-selectin primary antibody (CD62E, BBA16, R&D Systems, MN, USA), washed 3X with pre-warmed 1x PBS, labeled with an AF488-conjguated anti-mouse secondary antibody, and counterstained with DAPI in Prolong Gold. A secondary antibody only control was used for normalization. The fluorescently labeled cells were imaged using the same methods as in Section 2.7, except that NS were not visualized. The integrated intensity of the AF488 anti-mouse channel of each image was measured using ImageJ and normalized to the secondary only control to quantify E-selectin expression as a function of exposure time to TNF-α (Figure S5).

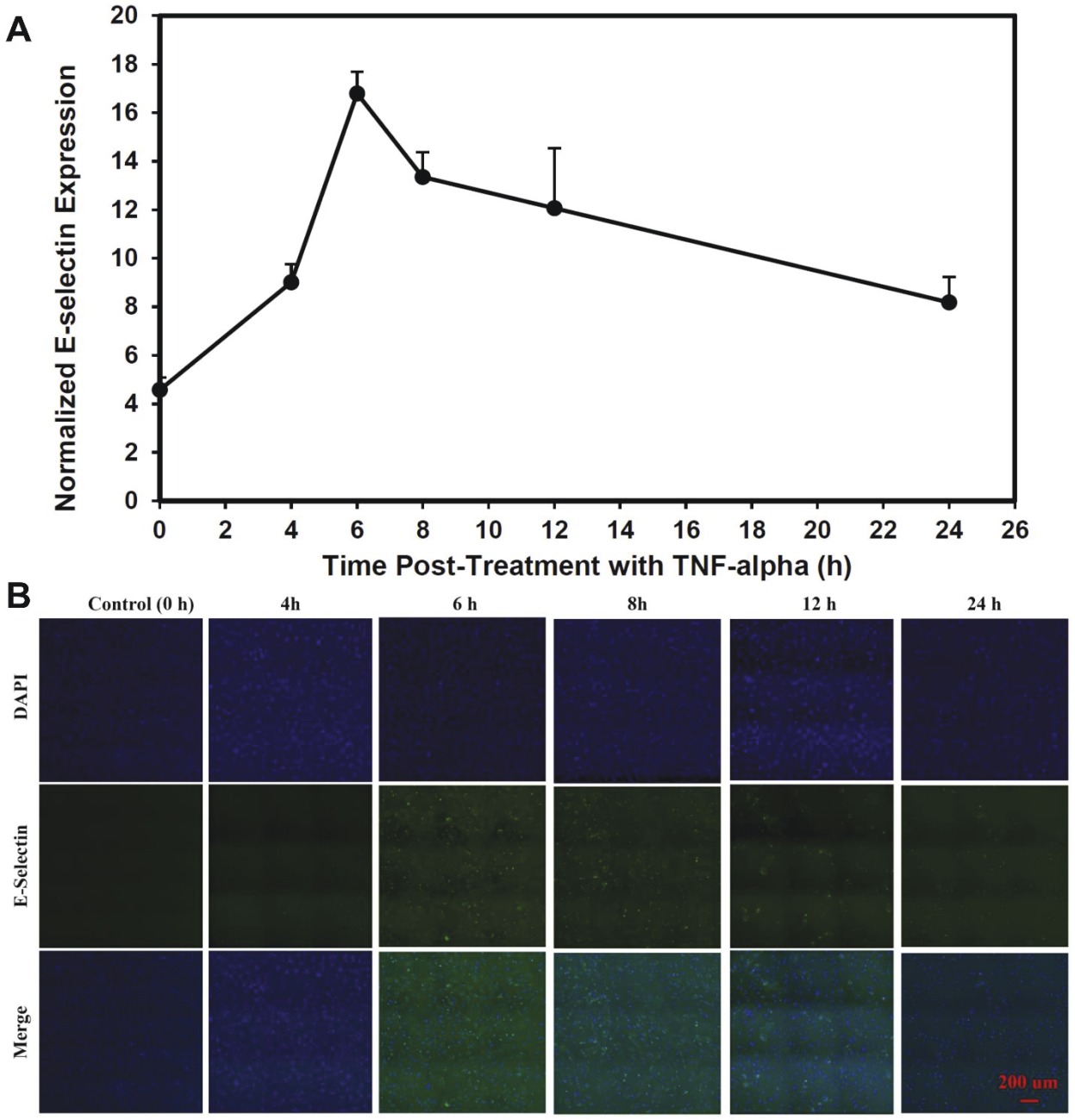

Figure S5. Temporal E-selectin Expression by HMVEC-Ls Post Exposure to 10 ng/ml TNF-α. (A) E-selectin expression was quantified via (B) immunofluorescence image intensity analysis (integrated intensity) as a function of exposure time to TNF-α. The measured integrated intensity for E-selectin was normalized to the secondary antibody only control. Based on these results, all experiments utilized a 6-hr treatment to induce inflammation.

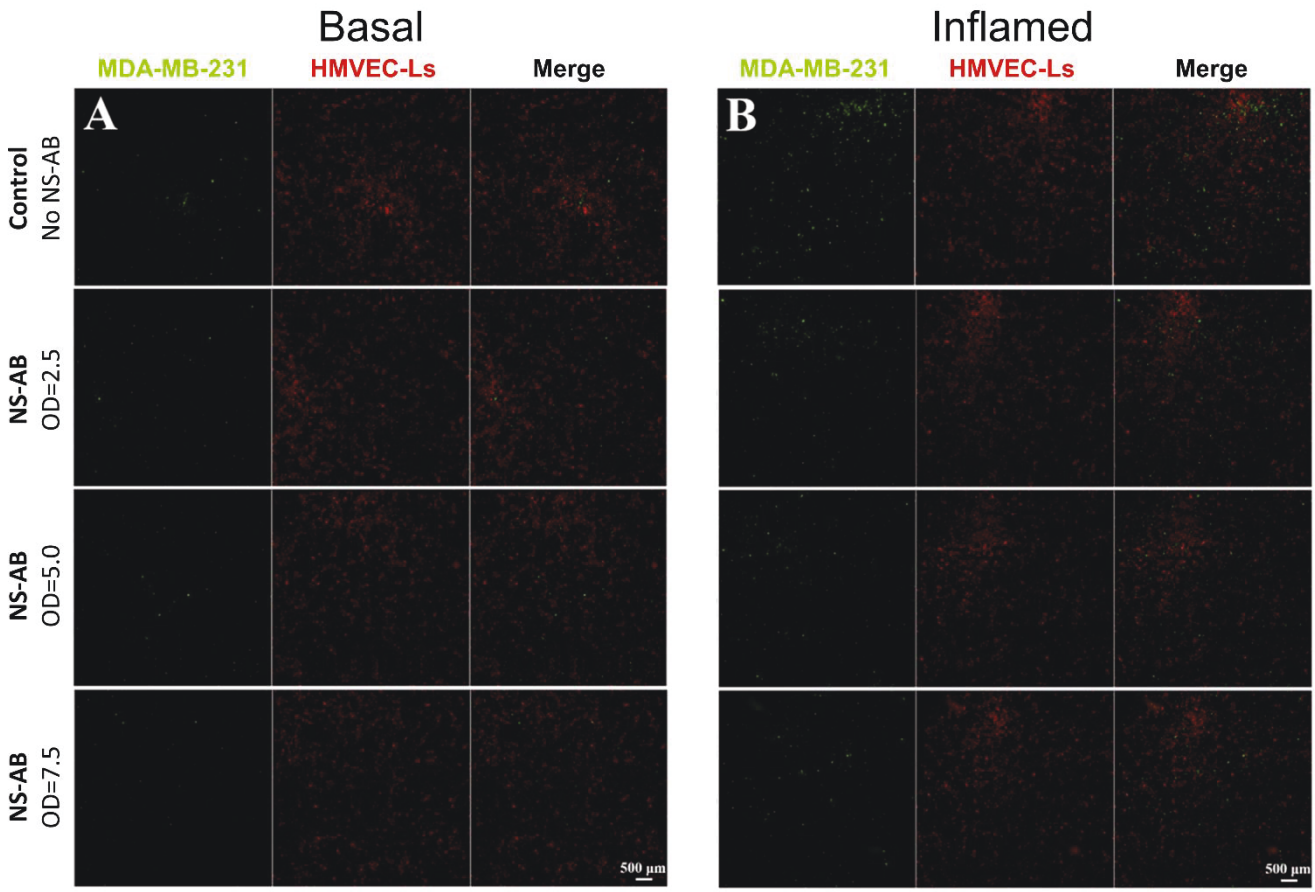

Figure S6. Inhibition of MDA-MB-231 Binding to HMVEC-Ls Using E-Selectin-Functionalized Nanoshells. Fluorescence microscopy images depicting GFP-expressing MDA-MB-231s bound to (A) basal or (B) inflamed HMVEC-Ls treated with E-selectin NS-AB at concentrations ranging from OD^{800nm}=0 (control: no NS) to OD^{800nm}=7.5. Red=HMVEC-Ls labeled with red cell tracker, Green=GFP-MDA-MB-231s.